NEURAL REGENERATION RESEARCH
September 2015, Volume 10, Issue 9
www.nrronline.org

RESEARCH ARTICLE

Transplantation of erythropoietin gene-modified neural stem cells improves the repair of injured spinal cord

Min-fei Wu[1], Shu-quan Zhang[2], Rui Gu[3,*], Jia-bei Liu[3], Ye Li[3], Qing-san Zhu[3]

1 Department of Orthopedics, the Second Hospital of Jilin University, Changchun, Jilin Province, China
2 Department of Orthopedics, Tianjin Nankai Hospital, Tianjin, China
3 Department of Orthopedics, China-Japan Union Hospital of Jilin University, Changchun, Jilin Province, China

***Correspondence to:**
Rui Gu, M.D., fandiliucl@126.com.

orcid:
0000-0003-4406-1553 (Rui Gu)

doi: *10.4103/1673-5374.165521*
http:*//www.nrronline.org/*

Accepted: *2015-08-17*

Abstract

The protective effects of erythropoietin on spinal cord injury have not been well described. Here, the eukaryotic expression plasmid pcDNA3.1 human erythropoietin was transfected into rat neural stem cells cultured *in vitro*. A rat model of spinal cord injury was established using a free falling object. In the human erythropoietin-neural stem cells group, transfected neural stem cells were injected into the rat subarachnoid cavity, while the neural stem cells group was injected with non-transfected neural stem cells. Dulbecco's modified Eagle's medium/F12 medium was injected into the rats in the spinal cord injury group as a control. At 1–4 weeks post injury, the motor function in the rat lower limbs was best in the human erythropoietin-neural stem cells group, followed by the neural stem cells group, and lastly the spinal cord injury group. At 72 hours, compared with the spinal cord injury group, the apoptotic index and Caspase-3 gene and protein expressions were apparently decreased, and the bcl-2 gene and protein expressions were noticeably increased, in the tissues surrounding the injured region in the human erythropoietin-neural stem cells group. At 4 weeks, the cavities were clearly smaller and the motor and somatosensory evoked potential latencies were remarkably shorter in the human erythropoietin-neural stem cells group and neural stem cells group than those in the spinal cord injury group. These differences were particularly obvious in the human erythropoietin-neural stem cells group. More CM-Dil-positive cells and horseradish peroxidase-positive nerve fibers and larger amplitude motor and somatosensory evoked potentials were found in the human erythropoietin-neural stem cells group and neural stem cells group than in the spinal cord injury group. Again, these differences were particularly obvious in the human erythropoietin-neural stem cells group. These data indicate that transplantation of erythropoietin gene-modified neural stem cells into the subarachnoid cavity to help repair spinal cord injury and promote the recovery of spinal cord function better than neural stem cell transplantation alone. These findings may lead to significant improvements in the clinical treatment of spinal cord injuries.

Key Words: *nerve regeneration; spinal cord injury; neural stem cells; erythropoietin; motor function; subarachnoid cavity; transplantation; injury; recovery; neural regeneration*

Funding: *This study was supported by the Science and Technology Development Program of Jilin Province of China, No. 2011084.*

Wu MF, Zhang SQ, Gu R, Liu JB, Li Y, Zhu QS (2015) Transplantation of erythropoietin gene-modified neural stem cells improves the repair of injured spinal cord. Neural Regen Res 10(9):1483-1490.

Introduction

The existing treatments for spinal cord injury (SCI) are unable to achieve the desired effect (Kim et al., 2012; Ercan et al., 2014). Neural regeneration after primary injury to the central nervous system is difficult, and the injury is often irreversible. In contrast, secondary injuries can be controlled and are reversible (Grimm et al., 2006). Neural stem cells (NSCs) continuously proliferate *in vitro*, self-renew, and can differentiate into neurons and astrocytes (Abbasnia et al., 2015). Thus, NSCs transplanted into rats after SCI can help recover their neurological functions (Cohen et al., 2015; Maiese et al., 2015).

Recently, the important functions of erythropoietin (EPO) in spinal repair have been increasingly recognized. Wu et al. (2015) reported that EPO has neuroprotective effects against hypoxic-ischemic brain injury, and human EPO (hEPO) has multiple biological effects and is important clinically (Wu et al., 2015).

NSC transplantation into the subarachnoid cavity allows the transplanted cells to quickly enter the nervous system and increases their survival rate (Mahmood et al., 2002). In the present study, hEPO was innovatively transfected into NSCs by gene transfection, the transfected NSCs were transplanted into the subarachnoid cavity of rats after SCI,

and the effects of the transfected NSCs on apoptosis and the recovery of lower limb motor function following SCI were assessed.

Materials and Methods

Experimental animals

A total of 12 Sprague-Dawley rat fetuses weighing 10–14 g were obtained from 1 female rat weighing 325 g at gestational day 14. The NSCs were collected from these rat fetuses. A total of 85 healthy male Sprague-Dawley rats weighing 200–250 g were used for the *in vivo* experiments. All rats were purchased from the Animal Laboratory of the Chinese Academy of Medical Sciences in China (license No. SCXK (Jin) 20090068). This study was approved by the Animal Ethics Committee of the Chinese Academy of Medical Sciences in China. All of the rats were housed under controlled conditions (22°C) in 12-hour light/dark cycles with free access to food and water. All surgeries were performed under anesthesia with 10% chloral hydrate 0.4 mL/100 g, and all efforts were made to minimize the pain and distress of the experimental animals. All of the animal procedures were conducted in accordance with the Guide for the Care and Use of Laboratory Animals as adopted and promulgated by the U.S. National Institutes of Health.

Culture, identification, and labeling of NSCs from rat brain tissues

NSC culture: The pregnant rat at gestational day 14 was euthanized by cervical dislocation, and then sterilized with 75% ethanol (Wang et al., 2011). The fetal rats were harvested by opening the abdomen. The brains of the fetal rats were immersed in Dulbecco's modified Eagle's medium (DMEM)/F12 medium (North of Shanghai Biological Technology Co., Ltd., Shanghai, China). After removing the meninges and blood vessels, the brain tissues were immersed in DMEM/F12 medium, triturated with a pipette, and filtered through a 100-mesh sieve. The suspension was then placed in a culture flask and incubated with epidermal growth factor (10 μg/mL; Sigma, St. Louis, MO, USA), basic fibroblast growth factor (10 μg/mL; Sigma), and N_2 additive (Sigma) in an incubator (RS Biotech, Irvine, UK) at 37°C and 5% CO_2 for 72 hours. The medium was then replaced.

NSC identification: Immunocytochemical staining was performed to identify NSCs. After 3 days of culture, the NSCs were seeded onto polylysine-coated coverslips. The neurospheres that formed were subjected to immunohistochemical staining for Nestin using a primary mouse anti-rat Nestin monoclonal primary antibody (Sigma; 1:200) at 4°C for 8 hours. The secondary antibody was fluorescein isothiocyanate-conjugated goat anti-mouse IgG (1:300; Boster, Wuhan, China). The cells were visualized using phase contrast microscopy (Olympus, Tokyo, Japan).

The identified NSCs were digested with 0.25% (1:4) trypsin and formed into a single cell suspension. The NSCs were then washed with serum-free DMEM/F12 medium, resuspended in 0.5 mL of diluent C at 2×10^7 cells/mL, and stained for immunofluorescence according to the CM-Dil staining kit protocol (Shanghai Qianchen Biological Technology Co., Ltd., Shanghai, China). An aliquot of 1×10^5 cells was washed with phosphate buffered saline (PBS; North of Shanghai Biological Technology Co., Ltd., Shanghai, China) immediately after labeling and fixed with 1% paraformaldehyde. After 24 hours of culture, the cells were visualized with a fluorescence microscope (Olympus).

hEPO transfection and western blot assay

As previously described (Yang et al., 2010), fourth passage NSCs were incubated in DMEM containing 10% fetal bovine serum in an incubator at 37°C and 5% CO_2. The NSCs were subcultured once every 3 days. NSCs in the logarithmic growth phase were seeded onto a 24-well plate at 6×10^4 cells/well and cultured for 3 days. The medium was discarded, and the NSCs were washed twice with PBS. Recombinant adeno-associated virus (rAAV) 2-hEPO diluted with serum-free, low glucose DMEM was added following a multiplicity of infection = 10^5 and incubated at 37°C for 2 hours. Sufficient amounts of fetal bovine serum and low glucose DMEM for 1 week were separately added. The cell culture medium was not replaced for 3 days prior to the western blot assay. Under the same conditions, normal control cells were transfected with empty vectors. Thus, two groups were set up during the rAAV2-hEPO transfection: a control group receiving an empty vector and an hEPO transfection group. The cell suspensions for each group were centrifuged at 300 × *g* for 5 minutes, and then the target cells were collected. Following removal of the medium, 400 μL of lysate was added to extract the total protein. The protein concentration was measured using the Bradford assay. The extracted proteins were electrophoresed on a 5% stacking gel at 40 V for 1 hour and 10% separating gel at 60 V for 3.5 hours before transfer to a polyvinylidene difluoride membrane using the wet method at 14 V for 14 hours. The membranes were blocked in a swing bed at 37°C for 2 hours, incubated with rabbit anti-human EPO polyclonal antibody (1:800; Santa Cruz Biotechnology, Santa Cruz, CA, USA) at 37°C for 2 hours, and washed four times in Tris-buffered saline with Tween 20 for 5 minutes each. The membranes were then incubated with goat anti-rabbit antibody (1:700; BD, Pharmingen, San Diego, CA, USA) at 37°C for 1.5 hours, washed four times in Tris-buffered saline with Tween 20 for 5 minutes each, and visualized with dimethylbenzidine. The experiment was repeated in triplicate. Data were analyzed using the Quantity One image analysis system (Bio-Rad, Hercules, CA, USA). Protein expression levels are reported as the optical density ratio of the target protein to glyceraldehyde phosphate dehydrogenase (GAPDH).

Animal models of spinal cord injury and cell transplantation

A total of 85 healthy female Sprague-Dawley rats were acclimatized for 2 weeks, anesthetized with an intraperitoneal injection of 2.5% ketamine 20 mg/kg, and secured on a bench in the prone position. The lower back was shaved. A median incision was made on the back centered on the $T_{8–9}$ spinous

Table 1 Primer sequence

Primer	Sequence	Product size (bp)	Temperature (°C)
bcl-2	Upstream: 5'-CTG GTG GAC AAC ATC GCT CTG-3' Downstream: 5'-GGT CTG CTG ACC TCA CTT GTG-3'	228	55
Caspase-3	Upstream: 5'-GAA CGC GAA GAA AAG TGA CC-3' Downstream: 5'-AGC CCA TTT CAG GGT AAT CC-3'	156	55
GAPDH	Upstream: 5'-AGT ATG ACT CCA CTC ACG GCA A-3' Downstream: 5'-TCT CGC TCC TGG AAG ATG GT-3'	100	55

GAPDH: Glyceraldehyde phosphate dehydrogenase.

Table 2 Motor function as assessed by the BBB and inclined plane test scores in SCI rats

		Time after injury					
Group	Before injury	1 day	3 days	1 week	2 weeks	3 weeks	4 weeks
BBB score							
SCI	21.00±0.00	0.00±0.00	1.52±0.23	2.75±0.89	8.35±1.56	11.24±2.23	13.64±1.20
NSCs	21.00±0.00	0.00±0.00	2.71±0.36	4.58±0.32	10.6±2.62	12.66±1.98	15.66±1.18
hEPO-NSCs	21.00±0.00	0.00±0.00	3.80±0.47	6.98±0.43	12.82±2.63	15.62±2.24	17.56±0.35
Inclined plane test (°)							
SCI	42.34±2.23	15.62±2.34	16.9±2.43	20.14±3.52	23.56±4.20	26.47±2.75	28.42±2.55
NSCs	42.52±3.80	15.68±2.79	19.20±3.22	25.24±4.72	30.42±6.32	32.83±3.05	36.74±2.47
hEPO-NSCs	42.53±3.21	15.83±3.32	23.58±3.52	29.27±6.25	33.7±5.18	36.67±4.45	40.37±3.32

At 1–4 weeks post injury, significant differences in the inclined plane test and modified BBB scores were detected at the same time point between groups ($P < 0.05$; mean ± SD, $n = 5$, one-way analysis of variance and the least significant difference test). SCI: Spinal cord injury; NSCs: neural stem cells; hEPO: human erythropoietin; BBB: Basso, Beattie, and Bresnahan locomotor scale.

process to expose the $T_{7–10}$ spinous processes and the lamina. The $T_{8–9}$ spinous process and part of the lamina tissue were removed. This exposed spinal cord tissue defined the lesion area. Using a modification of Allen's method (Verstraete et al., 2014; Lai et al., 2015), a 10-g object was dropped from a vertical height of 2.5 cm that directly impacted the rat spinal cord. Paralysis of the lower limbs was observed after impact as the rat tail experienced swings and spasms, suggesting successful establishment of the model. The wound was then washed with penicillin saline, and the tissues were sutured closed in layers.

Abdominal massage and extrusion were performed in the morning and afternoon daily to assist urination. A total of 69 rats with SCI were established, and those were randomly assigned to the SCI, NSCs, or hEPO gene-modified NSCs (hEPO-NSCs) groups.

Six hours after SCI, a 1-cm longitudinal incision was made centered on the T_5 spinous process by cutting the skin and fascia and dissociating the bilateral paraspinal muscles to expose the L_3 spinous process and vertebral plate. The L_3 spinous process and vertebral plate were then removed to expose the $L_{3–4}$ spinal dura mater. A microsyringe was used to gently pierce the spinal dura mater with the tip parallel to the vertebral canal. The needle was slowly inserted in the direction of the rat head until cerebrospinal fluid was observed upon pumpback. In the SCI group, 20 μL of DMEM/F12 medium was infused into the subarachnoid cavity. In the NSCs group, 20 μL of DMEM/F12 medium (2×10^4 cells/μL) was infused into the subarachnoid cavity. In the hEPO-NSCs group, 20 μL of DMEM/F12 medium (2×10^4 cells/μL) (Wang et al., 2015) was slowly infused into the subarachnoid cavity over 5 minutes.

In each group, five rats were used for the terminal dexynucleotidyl transferase(TdT)-mediated dUTP nick end labeling (TUNEL) assay, five for reverse transcription-polymerase chain reaction (RT-PCR), five for hematoxylin-eosin staining and CM-Dil counting, five for the horseradish peroxidase (HRP) tracer experiment, five for detection of motor function (three for CM-Dil fluorescence and hematoxylin-eosin staining, two for HRP retrograde tracing), and six for the electrophysiological evaluations (two for CM-Dil fluorescence and hematoxylin-eosin staining, one for HRP retrograde tracing, and only three for the electrophysiological evaluation).

TUNEL assay for apoptosis in the rat spinal cord

At 72 hours post injury, each rat was anesthetized with chloral hydrate. The chest was opened, and the rat was fixed with 4% paraformaldehyde after aortic cannulation through the left ventricle. With the injured spinal cord as the center point, 2 cm of spinal cord was harvested and fixed with paraformaldehyde, and paraffin sections were prepared. The paraffin sections were dewaxed, and the cells were quantified by TUNEL assay following the kit instructions (Perchem, Shanghai, China). A total of 500 μL of TUNEL reaction mixture was prepared by adding 50 μL of enzyme solution to 450 μL of marking fluid. After centrifugation and mixing, the samples were washed twice in PBS. The sample and positive control sections were separately

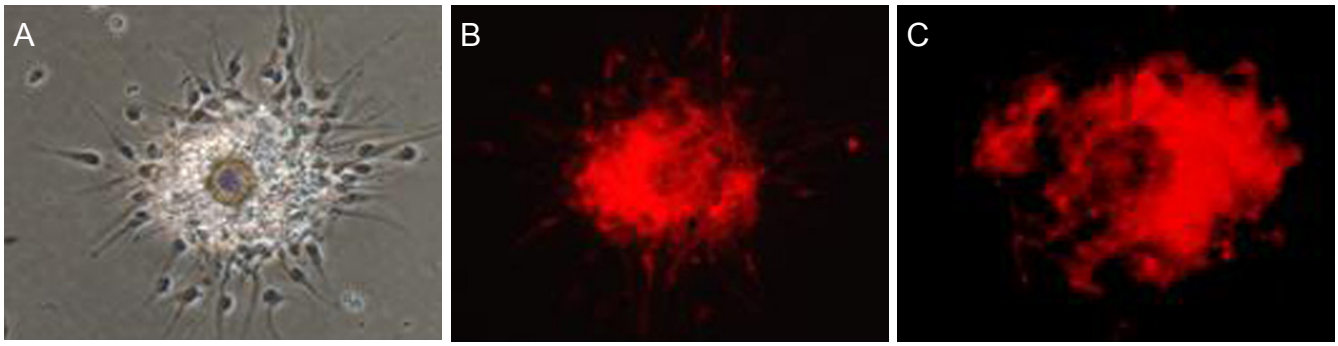

Figure 1 Culture, identification, and labeling of neural stem cells (NSCs).
(A) Morphology of primary NSCs by inverted phase contrast microscopy (× 40); (B) NSCs positive for Nestin (immunofluorescence staining, × 40, red); (C) CM-Dil-positive NSCs (× 100; red).

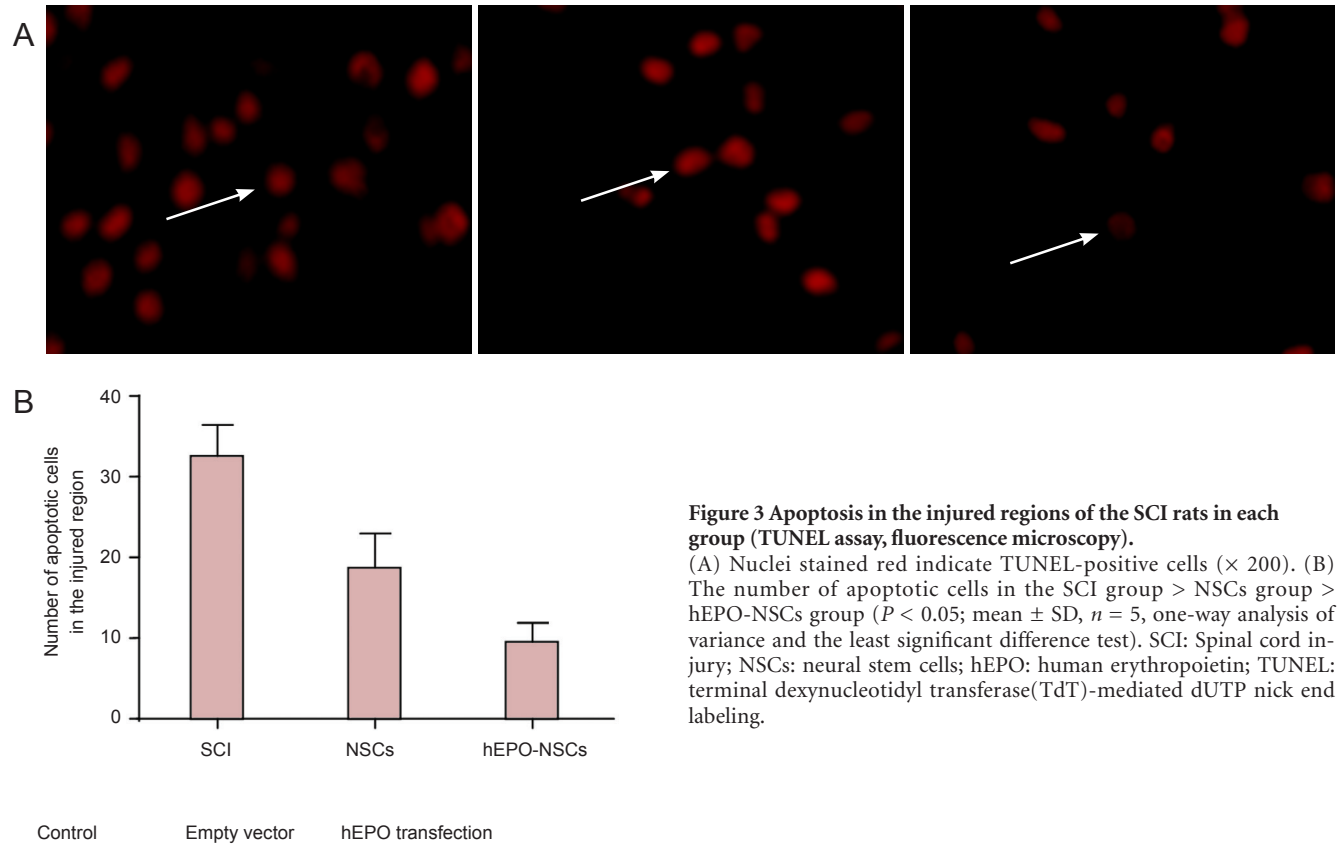

Figure 3 Apoptosis in the injured regions of the SCI rats in each group (TUNEL assay, fluorescence microscopy).
(A) Nuclei stained red indicate TUNEL-positive cells (× 200). (B) The number of apoptotic cells in the SCI group > NSCs group > hEPO-NSCs group ($P < 0.05$; mean ± SD, $n = 5$, one-way analysis of variance and the least significant difference test). SCI: Spinal cord injury; NSCs: neural stem cells; hEPO: human erythropoietin; TUNEL: terminal dexynucleotidyl transferase(TdT)-mediated dUTP nick end labeling.

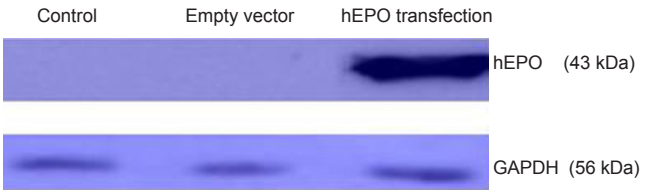

Figure 2 hEPO protein expression by NSCs in each group after 48 hours of transfection.
EPO protein expression by NSCs in the hEPO transfection group was apparent, but absent in the control and empty vector groups. hEPO: Human erythropoietin; NSCs: neural stem cells; GAPDH: glyceraldehyde phosphate dehydrogenase.

treated with 50 μL of TUNEL reaction mixture, while the negative control sections were treated with 50 μL of marking fluid without the enzyme solution. All sections were incubated in a wet box in the dark at 37°C for 60 minutes, washed three times in PBS, and imaged using a fluorescence microscope (Olympus, Tokyo, Japan) after adding a drop of PBS. The excitation wavelength was 450–500 nm. The range of emission was 515–565 nm. The cells were quantified in a 200× magnification field in ten sections from each group, and the average values were calculated.

RT-PCR

At 72 hours post injury, 50 mg of spinal cord was harvested from the injured region (Yi et al., 2005). Following the Trizol kit (Invitrogen Life Technologies, Carlsbad, CA, USA) instructions, the total RNA was extracted from the spinal

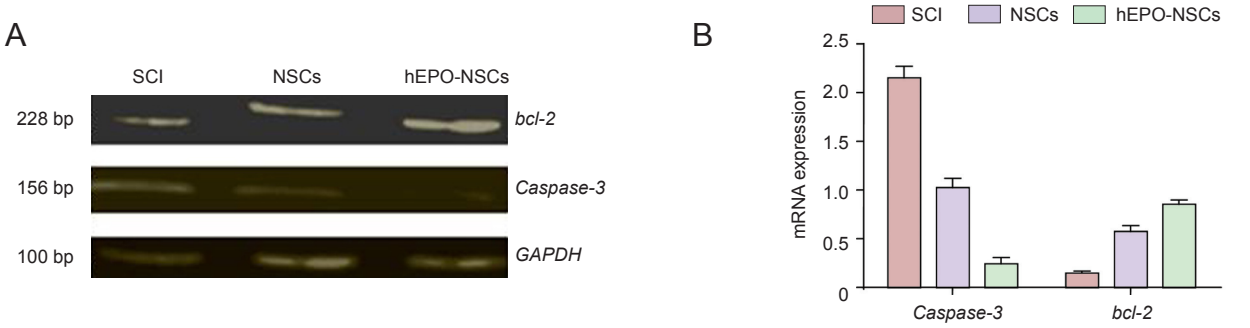

Figure 4 *bcl-2* and *Caspase-3* mRNA expression in the injured regions of the SCI rats in each group.
(A) Compared with the SCI group, *Caspase-3* gene expression was obviously lower, but *bcl-2* gene expression was higher in the hEPO-NSCs group. (B) Significant differences in the relative optical density values (/GAPDH) for both the *Caspase-3* and *bcl-2* mRNA expression levels were detected between groups ($P < 0.05$; mean ± SD, $n = 5$, one-way analysis of variance and the least significant difference test). SCI: Spinal cord injury; hEPO: human erythropoietin; NSCs: neural stem cells; GAPDH: glyceraldehyde phosphate dehydrogenase.

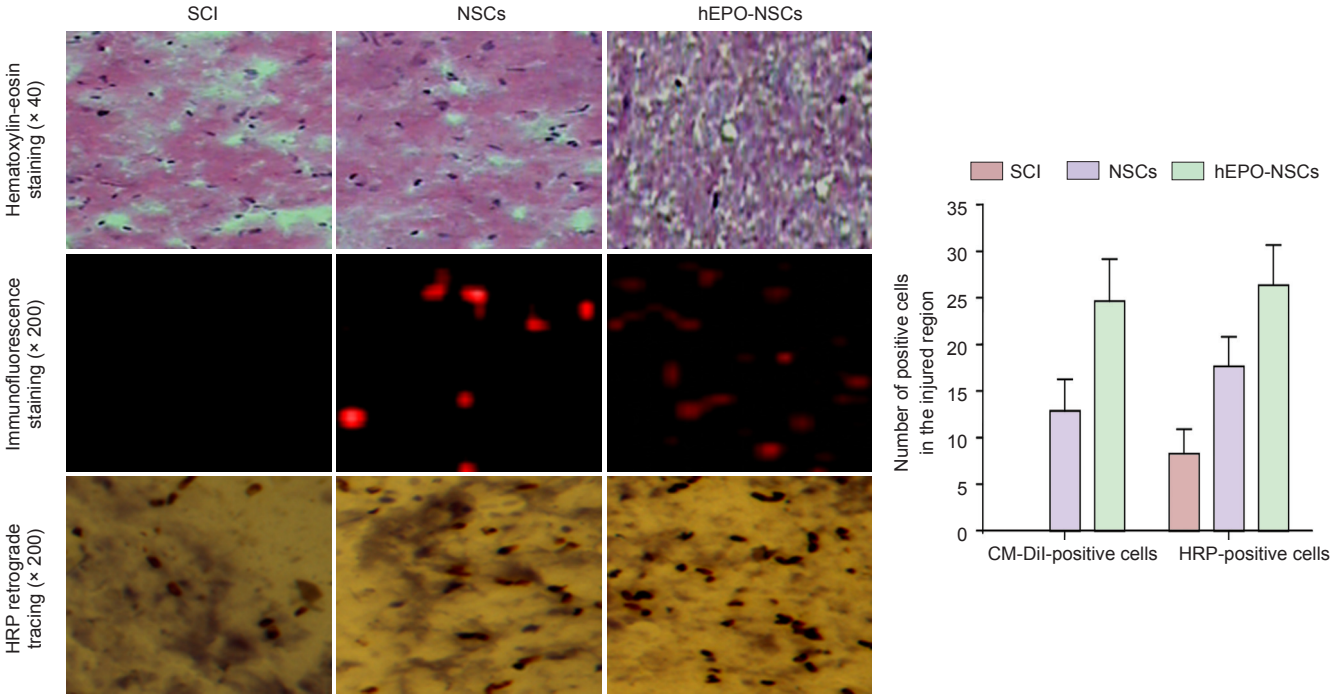

Figure 5 Pathological changes in the injured regions of the SCI rats from all groups.
Hematoxylin-eosin staining showed that a cavity formed in the spinal cord of the SCI group. The cavity was small in the NSCs group, but had nearly disappeared in the hEPO-NSCs group. The numbers of CM-DiI-positive cells and HRP-positive nerve fibers were larger in the hEPO-NSCs group than in the NSCs group, and smallest in the SCI group ($P < 0.01$; mean ± SD, $n = 5$, one-way analysis of variance and the least significant difference test). SCI: Spinal cord injury; NSCs: neural stem cells; hEPO: human erythropoietin; HRP: horseradish peroxidase.

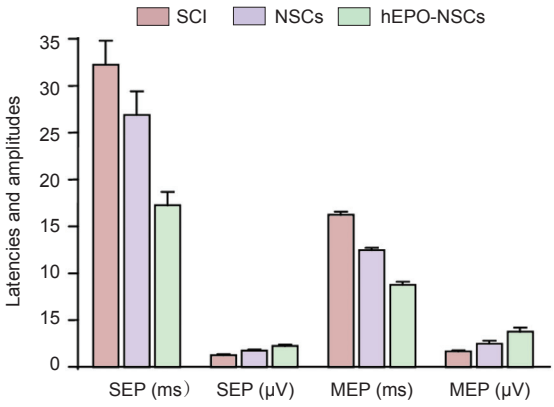

Figure 6 Detection of SEP and MEP in rats from each group at 4 weeks post injury.
Significant differences in the latencies and amplitudes of SEP and MEP were detected between groups ($P < 0.05$; mean ± SD, $n = 6$, one-way analysis of variance and the least significant difference tests). SCI: Spinal cord injury; hEPO: human erythropoietin; NSCs: neural stem cells; SEP: somatosensory evoked potential; MEP: motor evoked potential.

cord samples. The amount of total RNA was determined using an ultraviolet spectrophotometer. The mRNA was reverse-transcribed into cDNA using a two-step RT-PCR kit (TaKaRa), and then the cDNA was amplified by PCR. The primers used are shown in **Table 1**. The best primers for bcl-2 and Caspase-3 were identified using GenBank data and Primer 5.0 software (http://pga.mgh.harvard.edu/primerbank/). The primers were synthesized by Sangon Biotech (Shanghai) Co., Ltd. (Shanghai, China) after comparisons using the Basic Local Alignment Search Tool. The amplified products were electrophoresed, and a gel image analysis system (Beijing Wuyejia Technology Co., Ltd., Beijing, China) was used to determine the optical density. The integrated optical density ratio of bcl-2 and Caspase-3 to GAPDH was calculated.

Motor function and electrophysiological assessment

Before injury and at 1 and 3 days and 1, 2, 3, and 4 weeks after injury, the motor function in the lower limbs was assessed using an inclined plane test and the Basso, Beattie, and Bresnahan (BBB) locomotor scale. The range of BBB scores was between 0 (complete paralysis) and 21 (normal). The number and range of motion, weight loading, coordination of forelimb and hindlimb, and motion of the forepaw, hindpaw, and tail were assessed (Wang et al., 2013). For the inclined plane test, the rats were placed horizontally on a smooth tiltboard. From the horizontal position (0°), the angle of the board was increased 5° every attempt. The maximum angle at which the rats remained on the board for 5 seconds was recorded. The evaluation was started at 8:00 a.m. and was conducted by two investigators blinded to the group assignments.

At 4 weeks post injury, six rats were selected from each group. As previously described (Vaquero et al., 2006), a Keypoint 4 induced potential instrument (Beijing Weidi Kangtai Medical Instrument Co., Ltd., Beijing, China) was applied to measure the somatosensory evoked potentials and motor-evoked potentials. The rats were anesthetized with an intraperitoneal injection of 10% chloral hydrate, and then laid on the horizontal plane. The hind limbs were stimulated with a stimulating electrode, while a recording electrode was placed under the scalp at the intersection of the sagittal suture and coronal suture healing line (*i.e.*, the hindlimb cortical sensory area). A reference electrode was also placed 0.5 cm posterior to the hindlimb cortical sensory area. Direct current, square wave, electrical pulses were applied until the hind limb exhibited a slight tic. The test conditions included a pulse width of 0.2 ms, current intensity of 5–15 mA, and frequency of 3 Hz that was superimposed 50–60 times. Neurophysiological recovery was assessed by recording alterations in the somatosensory evoked potential amplitude and latency and by detecting the motor-evoked potential amplitudes and latencies. These parameters were obtained after anesthesia by placing the stimulating electrodes under the scalp 2 mm anterior to the coronal suture and 2 mm lateral to the sagittal suture (*i.e.*, in the motor cortex) and using a pulse width of 0.1 ms, stimulus intensity of 40 mA, and frequency of 1 Hz that was superimposed 300–500 times at a scanning speed of 5 ms/D and sensitivity of 5 μV/D.

Hematoxylin-eosin and CM-Dil fluorescence staining

At 4 weeks post injury, sections of the injured spinal cord were prepared for histological examination, fixed with 4% paraformaldehyde, sliced as frozen sections, and imaged using fluorescence microscopy (Wang et al., 2015) at 200× magnification. Ten fields from each section were observed to quantify the number of CM-Dil-positive cells per field, and the average value was used to calculate the number of CM-Dil-positive cells for each group (Wang et al., 2015).

HRP retrograde tracing

First, HRP was dissolved in physiological saline. After inducing anesthesia, the spinal cord of the rats was exposed. A solutions of 50% HRP (1 μL) was injected at 0.1 μL/10 min into the region 1 mm left and right of the T_{12} spinal dorsal median vein. The injection needle depth was 1.5 mm, and the needle was maintained in place for 15 minutes. After 3 days, the rats were anesthetized with chloral hydrate, and their hearts were perfused with 4% paraformaldehyde. The spinal cord $T_{3–11}$ segments were immersed in 30% sucrose solution at 4°C for 20 hours, and then cut into 5-μm-thick frozen sections. The sections were visualized with 3,3′-diaminobenzidine. Ten sections were randomly selected from each group, and the number of HRP-positive nerve fiber bundles on the spinal cord cross-sections was calculated using light microscopy imaging (Olympus) at 200× magnification (/mm^3). The average value was also calculated.

Statistical analysis

Measurement data are expressed as the mean ± SD. All data were analyzed using SPSS 17.0 software (SPSS, Chicago, IL, USA). The differences among multiple groups were compared using one-way analysis of variance and the least significant difference test. *P*-values less than 0.05 were considered statistically significant.

Results

***In vitro* culture, identification, and labeling of NSCs**

After 1 day of culture, the number of NSCs was increased, but the cells were small and irregularly shaped. A small part of the cell mass was adhered to the wall. After 5 days of culture, the number of NSCs was further increased, and the cells were large and spherical (**Figure 1A**). The immunofluorescence staining showed that the NSCs were strongly positive for Nestin (**Figure 1B**). The CM-Dil-positive NSCs appeared red under the fluorescence microscope (**Figure 1C**). The CM-Dil expression was stable in the cells, and the labeling rate was greater than 98%.

EPO expression in NSCs after transfection

The western blot assay indicated that 48 hours after the rAAV-mediated EPO gene transfection, EPO protein was being expressed by the NSCs in the hEPO transfection group, but not by the control or empty vector cell groups. This indicated that the hEPO gene was stably integrated in

the NSCs in the hEPO transfection group, and they maintained a stable expression of the target protein (**Figure 2**).

Apoptosis in the injured region of SCI rats after transfection

The TUNEL staining showed specific brown particles in the nuclei of apoptotic NSCs. Under light microscopy, the apoptotic cells were scattered all around the injured region and its edge. Significantly fewer apoptotic cells were found in the NSCs group than in the SCI group in the 200× fields ($P < 0.05$), and the smallest number of apoptotic cells was found in the hEPO-NSCs group ($P < 0.05$; **Figure 3**).

***bcl-2* and *Caspase-3* mRNA expression in the injured regions of SCI rats after transplantation of hEPO gene-modified NSCs into the subarachnoid cavity**

The RT-PCR results showed that at 72 hours after SCI, more *Caspase-3* mRNA expression in the spinal cord was found in the NSCs group than in the hEPO-NSCs group ($P < 0.05$). The *bcl-2* mRNA expression was lower in the NSCs group than in the hEPO-NSCs group ($P < 0.05$). In addition, the *Caspase-3* mRNA expression was significantly lower in the NSCs group than in the SCI group ($P < 0.05$), but the *bcl-2* mRNA expression was higher in the NSCs group than in the SCI group ($P < 0.05$; **Figure 4**).

Changes in motor function in SCI rats after transplantation of hEPO gene-modified NSCs into the subarachnoid cavity

No significant differences in inclined plane test or modified BBB scores were found among all of the rats before injury ($P > 0.05$). The inclined plane test and modified BBB scores were significantly higher in the NSCs and hEPO-NSCs groups than in the SCI group at 1–4 weeks after injury ($P < 0.05$). In addition, the inclined plane test and modified BBB scores were significantly greater in the hEPO-NSCs group than in the NSCs group at 1–4 weeks after injury ($P < 0.05$; **Table 2**).

Pathological changes in the injured regions of SCI rats after transfection

At 4 weeks post injury, the hematoxylin-eosin staining demonstrated changes to the spinal cord tissue at the injury site with a clear cavity, scarring, and structural disorder visible in the SCI group rats. These typical morphological changes to nerve cells were also observed in the transplanted region of the NSCs group rats. However, the cavity in the NSCs group was smaller than that in the SCI group, but larger than that in the hEPO-NSCs group. Typical nerve cell-like morphological changes were found in the hEPO-NSCs group, but no cavity was seen (**Figure 5**).

Scattered CM-Dil expression (red fluorescence) was found both in the NSCs and hEPO-NSCs groups, with less staining in the SCI group than that in the NSCs group, and the least amount of staining found in the hEPO-NSCs group ($P < 0.01$).

In the SCI group, 3 days after HRP injection through the intumescentia lumbalis and retrograde transportation, a few HRP-labeled nerve fibers were observed in the T_8 or higher segments. More HRP-positive nerve fibers were detected in the NSCs group than in the SCI group, and the largest number was found in the hEPO-NSCs group. In fact, many HRP-positive nerve fibers were seen in the hEPO-NSCs group. At 4 weeks post injury, significantly more HRP-positive nerve fibers were found in the hEPO-NSCs group than in the SCI group ($P < 0.01$).

Changes in somatosensory evoked potentials and motor evoked potentials in the rats after transfection

After inducing SCI in the rats, detection of the somatosensory evoked potentials and motor evoked potentials showed that the evoked potential waveforms had completely disappeared in the rats from every group. At 4 weeks post injury, the somatosensory and motor evoked potentials were slightly improved in the SCI group. The somatosensory and motor evoked potentials had noticeably recovered and the amplitudes increased. The latencies of the somatosensory and motor evoked potentials were smaller in the hEPO-NSCs group than in the NSCs group, and largest in the SCI group ($P < 0.05$). The amplitudes of the somatosensory and motor evoked potentials were larger in the hEPO-NSCs group than in the NSCs group, and smallest in the SCI group ($P < 0.05$). These results suggest that the conduction time for electrical signals from the hindlimb to the scalp was shorter in the hEPO-NSCs group than that in the SCI and NSCs groups. The conduction pathway was smooth and recovered well (**Figure 6**).

Discussion

NSCs can differentiate into nerve cells or glial cells, maintain the properties of stem cells after multiple passages, and survive in the body for extended periods of time after transplantation (Courtine et al., 2009; Chang et al., 2014; He et al., 2014). NSCs divide and proliferate at the transplantation site, and they can differentiate into the appropriate cells for a given local microenvironment as a substitute for the injured cells (Ung et al., 2008; Murray et al., 2010; Ren et al., 2013; Li et al., 2014). The transplantation of NSCs alone was not sufficient to fully repair injured spinal cord, suggesting that a combination of techniques is needed (Hasnan et al., 2013; Smithason et al., 2013).

EPO strongly inhibits neuronal apoptosis and the inflammatory reaction (Kristal et al., 2008; Recio et al., 2010; Seo et al., 2013; Zhong et al., 2013). Gorio et al. (2005) reported that the number of inflammatory cells in the injury site and surrounding area was clearly decreased and the neurological function was apparently recovered after EPO treatment. Previous studies have shown that EPO mitigates lipid peroxidation, reduces the degree of injury, suppresses the expression of excitatory amino acids, weakens the toxic effects, and protects neurons in SCI rats (Kaptanoglu et al., 2004; Lu et al., 2012). The results of the present study demonstrated that at 72 hours after injury, transplantation of hEPO gene-modified NSCs decreased *Caspase-3* mRNA and protein expression, and increased *bcl-2* mRNA and protein expression. In addition, *hEPO* mPRNA-modified NSCs transplantation decreased apoptosis, promoted spinal cord repair, increased the numbers of CM-Dil-positive cells and HRP-positive nerve

fibers, and contributed to the recovery of hindlimb motor function in SCI rats.

Acknowledgments: *We are very grateful to Doctor Bao-bin Liu from General Hospital of Tianjin Medical University in China for giving us rAAV2-hEPO expression vector.*

Author contributions: *MFW provided data, ensured the integrity of the data, wrote the paper, and was in charge of paper authorization. RG participated in study concept and design, and obtained the funding. SQZ analyzed the data. JBL was responsible for statistical analysis. YL and QSZ provided technical support and served as a principle investigator. All authors approved the final version of the paper.*

Conflicts of interest: *None declared.*

References

Abbasnia K, Ghanbari A, Abedian M, Ghanbari A, Sharififar S, Azari H (2015) The effects of repetitive transcranial magnetic stimulation on proliferation and differentiation of neural stem cells. Anat Cell Biol 48:104-113.

Chang R, Wang Y, Chang J (2014) LPS preconditioning ameliorates intestinal injury in a rat model of hemorrhagic shock. Inflamm Res 63:675-682.

Cohen SP, Hanling S, Bicket MC (2015) Epidural steroid injections compared with gabapentin for lumbosacral radicular pain: multicenter randomized double blind comparative efficacy study. BMJ 16:350.

Courtine G (2009) Transformation of nonfunctional spinal circuits into functional states after the loss of brain input. Nat Neurosci 12:1333-1342.

Du X, Yang XH, Wu YF (2015) Distribution of the cytoskeletal protein, Nestin, in acute leukemia. Biotech Histochem 90:384-394.

Ercan E, Bagla AG, Aksoy A (2014) In vitro protection of adipose tissue-derived mesenchymal stem cells by erythropoietin. Acta Histochem 116:117-125.

Gorio A, Madaschi L, Di Stefano B (2005) Methylprednisolone neutralizes the beneficial effects of erythropoietin in experimental spinal cord injury. Proc Natl Acad Sci U S A 102:16379-16384.

Grimm C, Wenzel A, Acar N (2006) Hypoxic preconditioning and erythropoietin protect retinal neurons from degeneration. Adv Exp Med Biol 588:119-131.

Hasnan N, Ektas N, Tanhoffer AI (2013) Exercise responses during functional electrical stimulation cycling in individuals with spinal cord injury. Med Sci Sports 45:1131-1138.

He K, Chen X, Han C (2014) Lipopolysaccharide-induced cross-tolerance against renal ischemia-reperfusion injury is mediated byhypoxia-inducible factor-2ct-regulated nitric oxide production. Kidney Int 85:276-288.

Kaptanoglu E, Solaroglu I, Okutan O (2004) Erythropoietin exerts neuroprotection after acute spinal cord injury in rats: effect on lipid peroxidation and early ultrastructural findings. Neurosurg Rev 27:113-120.

Kim HJ, Oh JS, An SS (2012) Hypoxia-specific GM-CSF-overexpressing neural stem cells improve graft survival and functional recovery in spinal cord injury. Gene Ther 19:513-521.

Kristal B, Sela S, Tanhilevski O (2008) Epoetin-alpha: preserving kidney function via attenuation of polymorphonuclear leukocyte priming. Isr Med Assoc J 10:266-272.

La YC, Chen AM, Bai XJ, Song XZ, Xu WG (2005) The effect of bcl-xL gene transfection in vivo on the expression of Caspase-3 and neuroprotective function following spinal cord injury. Zhonghua Shiyan Waike Zazhi 22:984-986.

Lai D, Wang F, Yao X (2015) Human endometrial mesenchymal stem cells restore ovarian function through improving the renewal of germline stem cells in a mouse model of premature ovarian failure. J Transl Med 13:155.

Li WC, Jiang DM, Hu N (2013) Lipopolysaeeharide preconditioning attenuates. neuroapoptosis and improves functional recovery through activation of Nrf2 in traumatic spinal cord injury rats. Int J Neurosci 23:240-247.

Li WC, Jiang R, Jiang DM (2014) Lipopolysaecharide precondition-ing attenuates apoptotic processes and improves neuropathologic changes after spinal cord injury in rats. Int J Neurosci 124:585-592.

Lu PG, Hu SL, Hu R (2012) Functional recovery in rat spinal cord injury induced by hyperbaric oxygen preconditioning. Neurol Res 34:944-951.

Mahmood A, Lu D, Wang L (2002) Intracerebral transplantation of marrow stromal cells cultured with neurotrophic factors promotes functional recovery in adult rats subjected to traumatic brain injury. J Neurotrauma 19:1609-1617.

Maiese K (2015) Novel applications of trophic factors, Wnt and WISP for neuronal repair and regeneration in metabolic disease. Neural Regen Res 10:518-528.

Murray KC (2010) Recovery of motoneuron and locomotor function after spinal cord injury depends on constitutive activity in 5-HT2C receptors. Nat Med 16:694-700.

Recio AC, Felter CE, Schneider AC (2012) High-voltage electrical stimulation for the management of Stage III and IV pressure ulcers among adults with spinal cord injury: demonstration of its utility for recalcitrant wounds below the level of injury. J Spinal Cord Med 35:58-63.

Ren LQ, Wienecke J, Chen M (2013) The time course of serotonin 2C receptor expression after spinal transection of rats: an immunohistochemical study. Neuroscience 236:31-46.

Seo TB, Chang IA, Lee JH (2013) Beneficial function of cell division cycle 2 activity in astrocytes on axonal regeneration after spinal cord injury. J Neurotrauma 30:1053-1061.

Smithason S, Moore SK, Provencio J (2013) Low-dose lipopolysaccharide injection prior to subaraehnoid hemorrhage modulates delayed deterioration associated with vasospasm in subarachnoid hemorrhage. Acta Neurochir Suppl 115:253-258.

Ung RV (2008) Role of spinal 5-HT2 receptor subtypes in quipazine-induced hindlimb movements after a low-thoracic spinal cord transection. Eur J Neurosci 28:2231-2242.

Van Steenwinckel J (2008) Role of spinal serotonin 5-HT2A receptor in 2',3'-dideoxycytidine-induced neuropathic pain in the rat and the mouse Pain 137:66-80.

Vaquero J, Zurita M, Oya S (2006) Cell therapy using bone marrow stromal cells in chronic paraplegic rats: systemic or local administration. Neurosei Lett 398:129-134.

Verstraete S, Walters MA, Devroe S (2014) Lower incidence of post-dural puncture headache with spinal catheterization after accidental dural puncture in obstetric patients. Acta Anaesthesiol Scand 58:1233-1239.

Wang D, Zhang JJ, Ma JJ (2011) Neural stem cells transplantation with Nogo-66 receptor gene silencing to treat severe traumatic brain injury. Neural Regen Res 6:725-731.

Wang D, Fan YH, Zhang JJ (2013) Transplantation of Nogo-66 receptor gene-silenced cells of in a poly (D,L-lactic-co-glycolic acid) scaffold for the treatment of spinal cord injury. Neural Regen Res 8:677-685.

Wu YW, Gonzalez FF (2015) Erythropoietin: a novel therapy for hypoxic-ischaemic encephalopathy? Dev Med Child Neurol 3:34-39.

Yang C, Ji L, Yue W, Wang RY, Li YH, Xi JF, Xie XY, He LJ, Nan X, Pei XT (2010) Erythropoietin gene-modified conditioned medium of human mesenchymal cells promotes hematopoieticdevelopment from human embryonic stem cells. Zhongguo Shi Yan Xue Ye Xue Za Zhi 18:976-980.

Zhong Q, Mmfish M, Kowluru RA (2013) Transcription factor Nrf2-mediated antioxidant defense system in the development of diabetic retinopathy. Invest Ophthalmol Vis Sci 54:3941-3948.

Copyedited by McCarty W, Norman C, Wang J, Qiu Y, Li CH, Song LP, Zhao M